

A Nonvolatile Plasmonic Switch Employing Photochromic Molecules

Ragip A. Pala, Ken T. Shimizu, Nicholas A. Melosh, and Mark L. Brongersma*

Geballe Laboratory for Advanced Materials, Stanford University, Stanford, California 94305

Received March 27, 2008

ABSTRACT

We demonstrate a surface plasmon-polariton (SPP) waveguide all-optical switch that combines the unique physical properties of small molecules and metallic (plasmonic) nanostructures. The switch consists of a pair of gratings defined in an aluminum film coated with a 65 nm thick layer of photochromic (PC) molecules. The first grating couples a signal beam consisting of free space photons to SPPs that interact effectively with the PC molecules. These molecules can reversibly be switched between transparent and absorbing states using a free space optical pump. In the transparent (signal "on") state, the SPPs freely propagate through the molecular layer, and in the absorbing (signal "off") state, the SPPs are strongly attenuated. The second grating serves to decouple the SPPs back into a free space optical beam, enabling measurement of the modulated signal with a far-field detector. In a preliminary study, the switching behavior of the PC molecules themselves was confirmed and quantified by surface plasmon resonance spectroscopy. The excellent (16%) overlap of the SPP mode profile with the thin layer of switching molecules enabled efficient switching with power densities of ~ 6.0 mW/cm² in $1.5\ \mu\text{m} \times 8\ \mu\text{m}$ devices, resulting in plasmonic switching powers of 0.72 nW per device. Calculations further showed that modulation depths in excess of 20 dB can easily be attained in optimized designs. The quantitative experimental and theoretical analysis of the nonvolatile switching behavior in this letter guides the design of future nanoscale optically or electrically pumped optical switches.

The microelectronics industry has witnessed a continual progression toward more compact, high speed, and power efficient devices over the last five decades. Currently, one of the most daunting problems preventing significant further increases in processor speed are thermal and RC delay time issues associated with electronic interconnection. Whereas high-speed optical interconnection schemes may offer interesting new solutions around these problems, their implementation is hampered by the large size mismatch between electronic and dielectric photonic components. CMOS foundries will decrease feature sizes on a Si chip from 65 to 45 nm and, ultimately, 10 nm. This will further increase this size mismatch, as dielectric photonic devices are limited in size to hundreds of nanometers by the fundamental laws of diffraction. The use of nanometallic (plasmonic) structures may help bridge the size gap between the two technologies and enable an increased synergy between chip-scale electronics and photonics.

Optical modulators are key components for a chip-scale optical link,¹ and their development has recently experienced a number of important advances toward the realization of efficient, high-speed devices.²⁻⁴ Unfortunately, many of the traditional CMOS modulator approaches run into problems as the weak nonlinear optical effects in Si (e.g., free carrier

dispersion) exhibit poor scaling characteristics. For this reason, long interaction lengths or resonant cavity devices are needed to attain required modulation depths. For this reason, the demand is growing for innovative new approaches. Recently, surface plasmon-polariton (SPP) based circuit elements including waveguides,⁵⁻⁹ ring resonators,¹⁰ modulators,¹¹⁻¹³ and photodetectors¹⁴⁻¹⁶ have been proposed and successfully demonstrated, starting a new era in which seamless integration of electronics and photonics may be enabled by plasmonics.^{17,18} In this letter, we analyze the performance of an all-optical switch that combines plasmonics with photochromic (PC) materials. The nonvolatile optical switching behavior seen in PC devices may provide significant power advantages over typical optical switches in plasmonic circuitry, which need a continuous optical supply power.¹⁹ Similar to low-leakage electronic devices, these switches only draw power if there is a logic level transition. Because of its simple layout, the conclusions drawn about this device geometry are quite general and important for future more complex modulator designs.

SPPs are electron density waves propagating along the surface of a metal and are coupled to bound transverse magnetic (TM) electromagnetic waves. The electromagnetic field intensity associated with a SPP is highest at the metal surface and decays exponentially into the metal and the adjacent dielectric. The strong confinement of the field to

* Corresponding author. E-mail: brongersma@stanford.edu. Telephone: (650) 736-2152. Fax: (650) 725-4034.

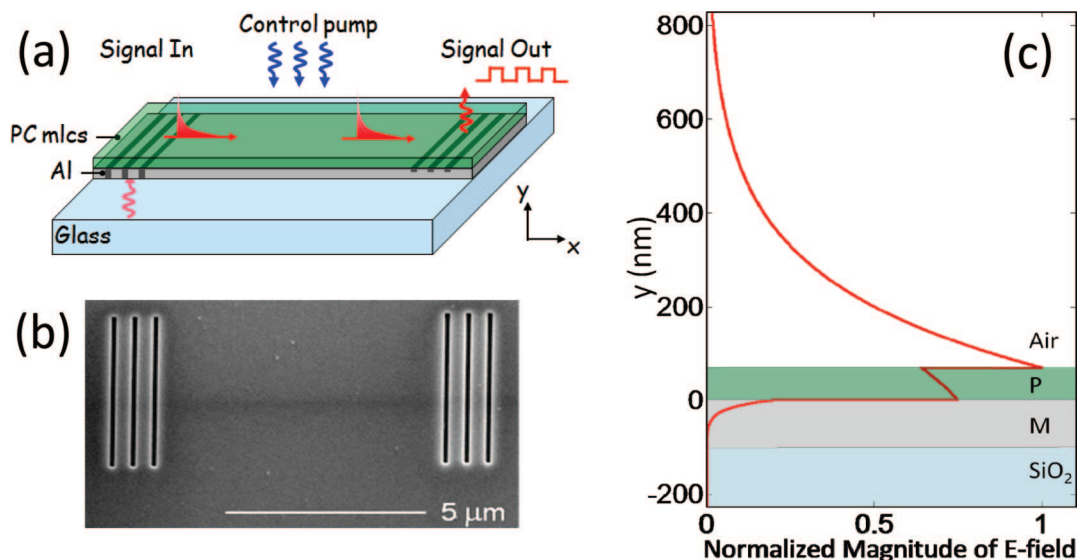


Figure 1. (a) Schematic of the plasmonic switching device. A signal beam is coupled to surface plasmon polaritons (SPPs) via the grating on the left and passes through a layer of photochromic molecules (PC mcs). A second grating on the right is used to decouple the SPPs back into free space photons, which are captured by a CCD camera. The PC molecules can be switched using a free space optical pump between the transparent and absorbing states and thereby turn the signal from “on” to “off”. (b) Scanning electron microscopy image of a switching device. (c) The SPP mode profile as calculated by the reflection pole method.

the surface renders the SPP propagation to be extremely sensitive to minor changes in the optical properties of materials in close proximity to the metal. This notion was already realized in the 1980s and led to a revolution in the development of ultrahigh sensitivity (bio)chemical sensors.²⁰ More recently, it was shown that the absorption spectra of nanometer thick organic films and even molecular monolayers sandwiched between two metal contacts can be determined by surface plasmon resonance spectroscopy (SPRS).²¹ Here, we demonstrate that the strong dependence of the SPP propagation length on absorption changes in an organic overlayer can be utilized to realize a compact plasmonic modulator. Photochromic compounds such as spiropyrans and spirooxazines,^{22,23} which exhibit strong reversible optical switching behavior between absorbing and transparent states are ideal candidates for a switching medium.

Figure 1a shows a schematic of the proposed plasmonic switching device. It consists of a pair of gratings defined in an aluminum film coated with PC molecules. Its intended operation can be described as follows. The grating on the left is designed to efficiently couple a signal beam to SPPs that propagate along the coated metal surface. The PC molecule coating can be switched between absorbing and transparent states using a free space optical pump. In the transparent state, the signal can freely propagate to the second grating, albeit with some Ohmic losses in the metal. In the absorbing state, the SPPs are much more strongly attenuated and the signal is switched from “on” to “off”. The second grating serves to couple the (non-absorbed) SPPs back into free space photons, enabling measurement of the modulated signal with a far-field detector.

It is by now well-established that grating structures can be used to efficiently couple a normally incident free space beam to SPPs and vice versa. If light hits a grating with a

grating constant, G , it can gain a momentum, $2\pi n/G$, in the direction of the periodicity, where n is an integer. This additional “momentum kick” enables the coupling of normally incident light (with no in-plane momentum) to SPPs, and the condition $k_{\text{spp}} = 2\pi/G$ is satisfied.²⁴ It has also been shown by Leveque²⁵ and Dittlbacher²⁶ et al. that an efficient coupling of about 20% can be achieved using a finite size grating through a careful choice of the grating dimensions.

Samples were prepared by first e-beam evaporating (Temesca) 20 nm thick titanium (Ti) and then 100 nm thick aluminum (Al) films on crystal quartz substrates that were cleaned in a piranha solution (30% H₂O₂, 70% H₂SO₄) at 90 °C and rinsed thoroughly with Millipore deionized water. Typical pressures during the metal evaporation were $5\text{--}7 \times 10^{-7}$ Torr. The grating structures were generated in the film using a focused ion beam tool, as shown in Figure 1b. The slits were 200 nm in width and 4 μm in length separated by a distance of 550 nm, which is slightly smaller than the surface plasmon wavelength, 625 nm, of the coated metal surface at the free space wavelength of 633 nm. These parameters were found to enable an efficient coupling to a free space signal beam, in agreement with previous reports.²⁴ The depth of the in- and out-coupling gratings were chosen to be 120 nm, etching all the way down to the glass substrate to allow an effective in-coupling and to eliminate any device variations in the out-coupled intensity due to uneven etching of the metal. The strongly absorbing Ti layer was used to remove any possible contributions to the modulated signal from bound modes excited at the metal–glass boundary; Theoretical calculations using the reflection pole method (RPM)²⁷ predict a 0.5 μm bound mode propagation distance, which is much smaller than the SPP propagation length on the top surface. Figure 1c shows the SPP field profile of the signal SPPs, as calculated by the RPM code. An excellent (16%) overlap of mode with the relatively thin (65 nm)

photochromic layer is observed. The overlap with the metal layer is more than 2 orders of magnitude smaller (0.15%), suggesting the possibility to attain a high modulation depth while minimizing resistive heating losses in the metal.

The active switching layer was fabricated by dissolving spiropyran molecules (5-methoxy-1,3,3-trimethylspiro [indoline-2,3'-[3H]naphtho[2,1-b]pyran]) into trace methanol and adding this mixture to a PMMA in chlorobenzene solution (MicroChem 495C). Typically, 10 wt % spiropyran in PMMA was used. Spiropyrans are PC molecules that can undergo a ring-opening reaction, as shown in Figure 2a. This particular molecule is thermodynamically stable in its transparent ring-closed state (I). Upon exposure to UV light, the ring opens (state II) and it becomes strongly absorbing. Heat or visible light can convert the absorbing ring-open state back to the transparent state, enabling photoinduced switching behavior. PMMA films with spiropyrans were spin-cast onto the Al film at 3×10^3 RPM for 60 s. The final films were 65 nm thick, as confirmed by SPR measurements and atomic force microscopy (AFM). The modulator devices were tested optically in a home-built optical analysis setup. A 633 nm He–Ne laser was used as the signal beam. Using a spatial filter, a beam with a Gaussian profile was created and focused onto the in-coupling grating using a 50 \times microscope objective. The grating effectively launched the SPPs toward the out-coupling grating, passing through the layer of PC molecules. The position of the sample was controlled by motorized stages with 10 nm placement accuracy. Another 50 \times long working distance objective was used to collect the signal from the out-coupling grating. The signal was visualized and quantified using a CCD camera (PIXIS, Princeton Instruments). For the modulation, 375 and 532 nm shutter-controlled CW solid state lasers were used, which were directed onto the sample through the out-coupling objective.

In a preliminary study, we analyzed the switching behavior (i.e., absorption changes) of the PC film on an Au substrate using a home-built SPRS spectroscopy tool. Details of such measurements are described elsewhere, and Figure 2b just illustrates the basic operation principle of the technique.²⁰ In brief, a monochromatic light beam is directed toward a metal coated glass slide through a glass prism. Index matching fluids between the glass slide and prism are used to minimize back reflections. The reflected light intensity is measured as a function of the incident angle. From the reflection curves, the real (n) and imaginary (k) part of the refractive index as well as the layer thicknesses (t) of the metal and PC coating can be determined. This is done by performing a least-squares fitting routine to the reflectivity curves predicted by the Fresnel equations for a multilayered system.

Figure 2c shows reflectivity curves for an Au film with the spiropyrans in the absorbing and transparent state at 633 nm. Both curves exhibit strong dips in the spectrum near 51 $^\circ$ due to significant energy transfer of light to SPPs. After the molecules were switched with a UV laser for 10 s, the dip became significantly broader, indicative of stronger absorption and a concomitant shorter SPP propagation length.

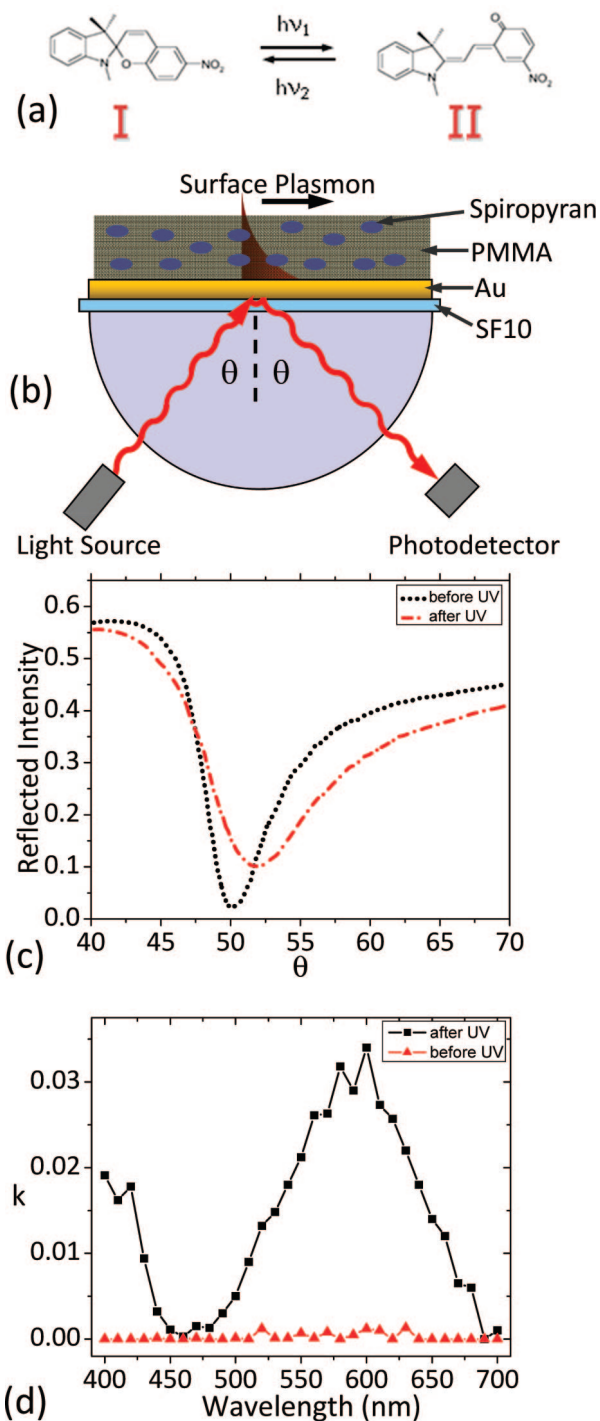


Figure 2. (a) Representation of a photochromic spiropyran molecule in its transparent ring-open and absorbing ring-closed forms. (b) Schematic of a prism coupling (Kretschmann) configuration used to determine reflectivity curves as a function of illumination angle. From the reflection curves the real (n) and imaginary (k) part of the refractive index of the metallic and photochromic layers can be determined. Light is coupled into a surface plasmon polaritons (SPPs) through a SF10 hemispherical prism. At a resonant angle, the light is converted into SPPs and a dip is observed in reflection. (c) Reflectivity curves taken at 633 nm from an Au film coated with a PMMA/spiropyran layer in the absorbing and transparent states. (d) Imaginary part of the refractive index as a function of wavelength, in the transparent (I) and absorbing states (II), as calculated from a least-squares fitting routine based on the Fresnel equations.

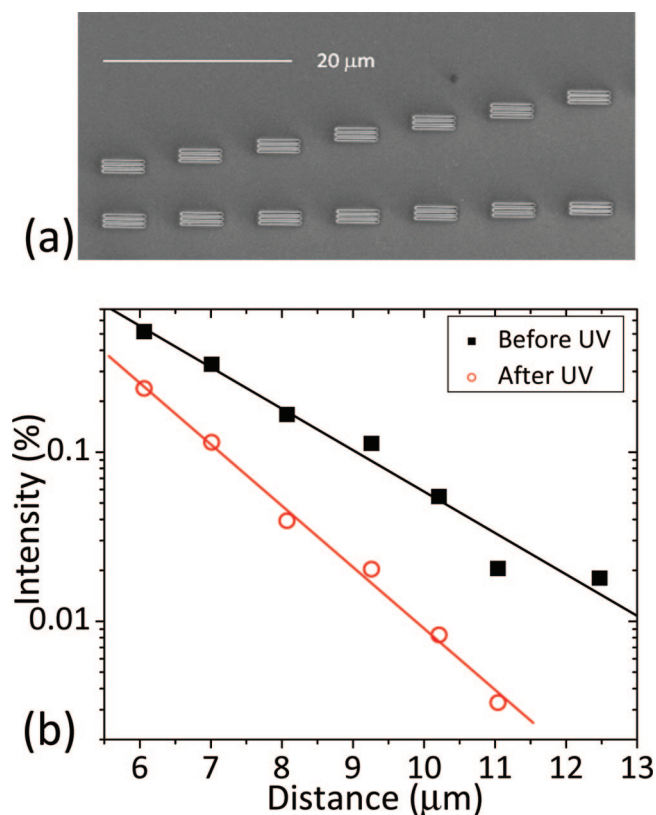


Figure 3. (a) Scanning electron microscopy image of sets of in- and out-coupling gratings used to determine the surface plasmon-polariton propagation length. The grating spacing was varied from 6 to 12 μm . (b) Measured out-coupled intensity as a function of grating spacing in the transparent and absorbing states of the photochromic molecules. The intensity was normalized to the in-coupled light intensity.

From these measurements, it is clear that the spiropyrans can be switched inside the PMMA layer on a metal film.

Figure 2d shows the dependence of k on wavelength in the transparent and absorbing states, obtained from reflectivity curves taken in the wavelength range from 400 to 700 nm. The substantial change in k from 0 to 0.035 at 600 nm is indicative of a large change in the absorption per unit length in this material, $\alpha = 4\pi k/\lambda$. On the basis of the modal overlap of the SPP with the switching layer and the changes in the k -value upon switching, an expected change in the SPP propagation distance can be calculated. For a switch with a fixed grating spacing, this change in propagation distance can in turn be used to calculate the modulation in the out-coupled signal intensity. To verify the predicted changes in propagation length, samples with pairs of in- and out-coupling gratings were generated with different inter-grating spacings in the range from 6 to 12 μm (see Figure 3a). By measuring the out-coupled intensity as a function of the grating spacing, the decay length of the SPP could be determined. Figure 3b shows the out-coupled light intensity at 633 nm as a function of grating spacing for samples in the transparent “on” and absorbing “off” states. The data were fit using an exponential fitting function of the form: $I_{\text{out}} = I_{\text{in}} \exp(-d/L_M) + B$, where I_{out} is the out-coupled light intensity, I_{in} is the initial intensity in-coupled intensity, d is the grating spacing, L_M is the measured decay length, and B

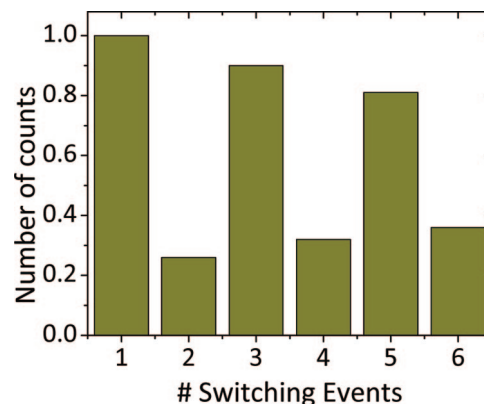


Figure 4. On and off switching behavior for a switching device with a grating spacing of 8 μm upon exposure to subsequent 375 and 532 nm laser beams.

is a background. In the fitting procedure, B was kept constant for the same set of measurements, while I_{in} and L_M were obtained from the best fit to the I_{out} vs d data. The measured decay lengths in the “on” and “off” states were $L_{M,\text{ON}} = 1.9 \pm 0.1$ and $L_{M,\text{OFF}} = 1.2 \pm 0.1$, respectively. This compares well to the predicted values of the decay lengths based on the measured changes in the magnitude of k by SPRS: $L_{C,\text{ON}} = 2.0 \pm 0.1$ and $L_{C,\text{OFF}} = 1.1 \pm 0.1$. The good agreement justifies our procedure to predict changes in the SPP decay length based on SPRS measurements and mode overlap calculations using the RPM method. Relatively straightforward SPRS measurements can therefore be used to identify and test promising switching materials.

Figure 4 shows reproducible on and off switching behavior for a fixed grating spacing of 8 μm . For this particular device, the switching layer was a 65 nm thick PMMA layer with 10 wt % spiropyrans. Initially, the layer was in the transparent state. Upon UV exposure, the out-coupled signal intensity saturated at 0.26 ± 0.02 of its original intensity, in good agreement with a calculated value of 0.23 ± 0.02 based on the change in k'' and the mode overlap. This corresponds to a modulation depth of 0.77 or -6 dB, as defined as the modulated signal intensity normalized by the signal in the transparent state of the PC molecules. Upon exposure with 532 nm green light, the signal goes back up to 0.90 of its original value. The incomplete recovery of signal is attributed to the degradation of the molecules and or the host matrix. A further reduction of the modulation is observed upon continued switching. Despite the observed degradation, this work provides a general pathway to identify, test, and predict the performance of switching materials. More robust, fast switching materials employing saturable absorbers or the quantum-confined Stark effect are promising candidates for future plasmonic switching devices.

The excellent (16%) overlap of the SPP mode profile with the strongly switching, active medium enabled complete switching with power densities of ~ 6.0 mW/cm² for 10 s. For our $1.5 \mu\text{m} \times 8 \mu\text{m}$ device, this enabled use of low ~ 0.72 nW switching laser powers and a total switching energy of 7.2 nJ/bit. The switching times and energies could potentially be significantly reduced by optimizing the host

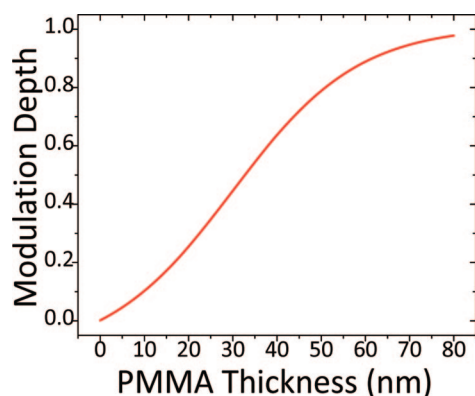


Figure 5. Calculated modulation depth as a function of the photochromic film thickness for an 8 μm long switching device as depicted in Figure 1a.

matrix for the PC molecules, providing a better switching environment. In the literature, PC molecules have been shown to repeatably switch within 20 ns.²⁸ Figure 5 shows that a high modulation depth switch can be realized with these photochromics. It shows the calculated dependence of the modulation depth on the film thickness calculated for a propagation distance of $d = 8 \mu\text{m}$ using the optical parameters of Al and the spiropyrans. The plot shows that modulation depths exceeding 20 dB or 99% for a 80 nm thick switching layer are feasible despite the small thickness of the switching layer. A more detailed theoretical analysis of the switching behavior will be published elsewhere.²⁹

In conclusion, we demonstrated a plasmonic switching device that exploits the unique optical switching properties of PC molecules and the strong modal confinement afforded by plasmonic waveguides. The switching behavior of PC molecules on a metal film was first demonstrated and quantified using surface plasmon resonance spectroscopy. From this work, it was found that an optical stimulus can induce a significant change in k'' (about 0.035) of the PC molecules. On the basis of the large degree of overlap (16%) of the SPP mode with the switching medium and the changes in k'' , a change in the SPP attenuation length from $L_{\text{C,ON}} = 2.0$ to $L_{\text{C,OFF}} = 1.1$ was predicted and verified using propagation length measurements. This enabled the realization of a prototype plasmonic switch with a modulation depth of 0.77 and a switching energy of 7.2 nJ/bit. A theoretical analysis further suggests modulation depths in excess of 20 dB are easy to attain, well in excess of previous modulator designs.

Acknowledgment. This work was supported by a MURI grant from the AFOSR (F49550-04-10437 and the grant from the DOE (F49550-04-10437).

References

- (1) Pavesi, L. A review of the various efforts to a silicon laser. In *Photonics Packaging and Integration III* Heyler, R. A., Robbins, D. J., Jabbour, G. E., Eds.; *Proc. SPIE* 2003, 4997, 206–220.
- (2) Lipson, M. *Nanotechnology* **2004**, 15, S622–S627.
- (3) Liu, A.; Jones, R.; Liao, L.; Samara-Rubio, D.; Rubin, D.; Cohen, O.; Nicolaescu, R.; Paniccia, M. *Nature* **2004**, 427, 615–618.
- (4) Kekatpure, R. D.; Brongersma, M. L. *Opt. Lett.* **2005**, 30, 2149–2151.
- (5) Takahara, J.; Yamagishi, S.; Taki, H.; Morimoto, A.; Kobayashi, T. *Opt. Lett.* **1997**, 22, 475–478.
- (6) Quinten, M.; Leitner, A.; Krenn, J. R.; Aussenegg, F. R. *Opt. Lett.* **1998**, 23, 1331–1333.
- (7) Weeber, J. C.; Dereux, A.; Girard, C.; Krenn, J. R.; Goudonnet, J. P. *Phys. Rev. B* **1999**, 60, 9061–9068.
- (8) Berini, P. *Phys. Rev. B* **2000**, 61, 10484–10503.
- (9) Zia, R.; Schuller, J. A.; Brongersma, M. L. *Phys. Rev. B* **2006**, 74, 165415.
- (10) Bozhevolnyi, S. I.; Volkov, V. S.; Devaux, E.; Laluet, J. Y.; Ebbesen, T. W. *Nature* **2006**, 440, 508–11.
- (11) Krasavin, A. V.; Zheludev, N. I. *Appl. Phys. Lett.* **2004**, 84, 1416–1418.
- (12) Pacifici, D.; Lezec, H. J.; Atwater, H. A. *Nat. Photonics* **2007**, xxx1.
- (13) Dintinger, J.; Robel, I.; Kamat, P. V.; Genet, C.; Ebbesen, T. W. *Adv. Mater.* **2006**, 18, 1645.
- (14) Ishi, T.; Fujikata, J.; Makita, K.; Baba, T.; Ohashi, K. *Jpn. J. Appl. Phys.* **2005**, 44, 364–366.
- (15) De Vlaminck, I.; Van Dorpe, P.; Lagae, L.; Borghs, G. *Nano Lett.* **2007**, 7, 703–706.
- (16) Yu, Z.; Veronis, G.; Fan, S.; Brongersma, M. L. *Appl. Phys. Lett.* **2006**, 89, 151116-1–151116-3.
- (17) Barnes, W. L.; Dereux, A.; Ebbesen, T. W. *Nature* **2003**, 424, 824–830.
- (18) Zia, R.; Schuller, J. A.; Brongersma, M. L. *Mater. Today* **2006**, 9, 20–27.
- (19) Tucker, R. S. *IEEE Photonics Technol. Lett.* **2007**, 19, 2036–2038.
- (20) Liedberg, B.; Nylander, C.; Sundstrom, I. *Sens. Actuators* **1983**, 4, 299.
- (21) Shimizu, K. T.; Pala, R. A.; Fabbri, J. D.; Brongersma, M. L.; Melosh, N. A. *Nano Lett.* **2006**, 6, 2797–2803.
- (22) Schaudel, B.; Guermeur, C.; Sanchez, C.; Nakatani, K.; Delaire, J. A. *J. Mater. Chem.* **1997**, 7, 61–65.
- (23) Berkovic, G.; Krongauz, V.; Weiss, V. *J. Mater. Chem.* **2000**, 10, 1741–1753.
- (24) Raether, H. *Surface Plasmon on Smooth and Rough Surfaces and on Gratings*; Springer-Verlag: Berlin, 1988.
- (25) Leveque, G.; Martin, O. J. F. *J. Appl. Phys.* **2006**, 100, 124301-1–124301-6.
- (26) Ditlbacher, H.; Krenn, J. R.; Hohenau, A.; Leitner, A.; Aussenegg, F. R. *Appl. Phys. Lett.* **2003**, 83, 3665.
- (27) Anemogiannis, E.; Glytsis, E. N.; Gaylord, T. K. *J. Lightwave Technol.* **1999**, 17, 929–940.
- (28) Sasaki, K.; Nagamura, T. *J. Appl. Phys.* **1998**, 83, 2894.
- (29) Pala R.; Brongersma, M. L. to be published.

NL0808839